

A Survey of High-Level Modeling and Simulation Methods for Modern Machine Learning Workloads

MICRO 2026 Submission – Confidential Draft – Do NOT Distribute!!

Anonymous Author(s)

Under Review

Anonymous

Abstract

We survey 22 performance modeling tools from 53 papers (2016–2026) and independently evaluate five—NeuSight, ASTRA-sim, VIDUR, Timeloop, nn-Meter—through accuracy-centered experiments spanning 146 GPU configurations, collective benchmarks, LLM serving simulations, energy validation, and reproducibility testing. Three findings emerge. First, self-reported accuracy is unreliable: NeuSight claims 2.3% MAPE but we measure 5.87–27.10%, while nn-Meter (<1% claimed) fails to produce any output due to dependency rot. Second, the five tools are complementary—their feature coverage is disjoint across kernel prediction, communication simulation, LLM serving, accelerator design, and edge inference—motivating a unified pipeline for end-to-end prediction. Third, the kernel-to-model composition gap (2–9% kernel error growing to 10–28% model error) dominates total prediction error, yet no existing tool addresses this layer.

Keywords

ML workload performance prediction, DNN accelerator modeling, GPU simulation, distributed training simulation, LLM inference serving, design space exploration, survey

1 Introduction

Domain-specific architectures [21, 27, 28] make performance prediction critical for ML workload deployment, yet no prior work examines *why* certain approaches succeed—analytical models [35, 49], trace-driven simulators [3, 72], hybrid approaches [40]—or how errors propagate across the abstraction stack; existing surveys focus on ML *techniques* for modeling [65] or specific hardware [49]. We contribute an **accuracy-centered verification framework** paired with an **LLM-focused benchmark suite**, replacing self-reported accuracy with reproducible evaluation showing claimed error rates are overstated by 2–4×:

- A **28-scenario LLM benchmark suite** spanning training and inference, revealing 50% of scenarios have zero tool support (Section 6).
- **Independent accuracy verification** of five tools (146 GPU configs, collectives, LLM serving, energy), showing self-reported claims are overstated (Section 7).
- A **unified simulation pipeline** identifying the kernel-to-model composition gap as the critical missing piece (Section 8).

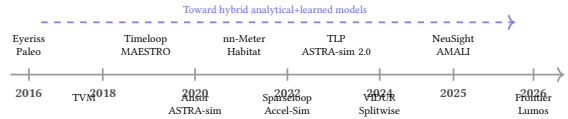


Figure 1: Evolution of performance modeling tools (2016–2026).

- A **coverage matrix** and research agenda for composition modeling, unified formats, and continuous validation (Sections 4, 9).

2 Survey Methodology

We searched ACM DL, IEEE Xplore, Semantic Scholar, and arXiv targeting architecture (MICRO, ISCA, HPCA, ASPLOS), systems (ML-Sys, OSDI, SOSP, NSDI), and related venues. From 287 candidates, 53 papers (2016–2026) plus 12 foundational works were classified by *methodology type*, *target platform*, and *abstraction level*. Prior surveys cover ML for processor DSE [56], DNN hardware [66], simulation infrastructure [4, 6, 61], and measurement [45, 59]; the closest work [14] compares edge predictors for NAS. We exclude proprietary tools (NVIDIA Nsight [48]), compiler cost models [37, 55, 67], and cluster schedulers [26, 54].

3 Background

ML workloads are computation graphs with statically known operator shapes amenable to analytical modeling; MoE and dynamic inference add input-dependent control flow [1, 51]. Performance depends on dataflow/tiling, KV cache [36], and compute–memory–network interactions; LLM inference splits into compute-bound prefill and memory-bound decode [2, 52, 74]. Five methodology types span accuracy–speed trade-offs: **analytical** [71] (μs), **cycle-accurate** [4, 31] (10^3 – 10^4 × slowdown), **trace-driven** [3, 72] (min.), **ML-augmented** [77] (ms), and **hybrid** [40, 75] (analytical+learned).

4 Taxonomy

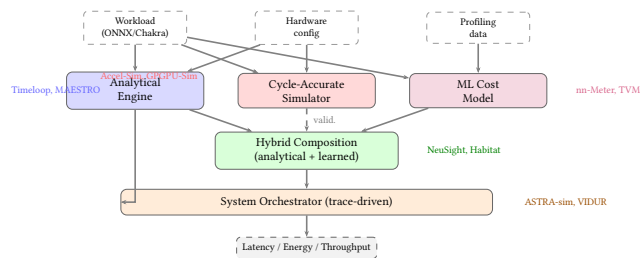
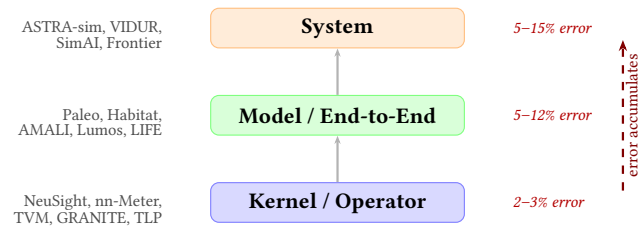
We organize the literature by *methodology type*, *target platform*, and *abstraction level* (Table 1).

Three gaps emerge (Figure 2): trace-driven replay is exclusive to distributed systems, edge devices lack hybrid alternatives, and no ML-augmented tool targets distributed settings.

Methodology–platform pairings. Platform constrains methodology: accelerators use analytical models [35, 49]; GPUs span all five types; distributed systems require trace-driven simulation [3, 72]; edge devices rely on ML-augmented [15, 77]; CPUs [47, 65] remain

Table 1: Methodology taxonomy: coverage matrix and trade-off profile. 0 = research gap.

Methodology	DNN Accel.	GPU	Distrib. Systems	Edge/ Mobile	CPU	Eval. Speed	Data Req.	Interp.	Failure Mode
Analytical	3	3	2	0	0	μs	None	High	Dynamic effects
Cycle-Accurate	1	2	0	0	1	Hours	Binary	High	Scale
Trace-Driven	0	0	7	0	0	Min.	Traces	Med.	Trace fidelity
ML-Augmented	0	3	0	3	1	ms	Profiling	Low	Distrib. shift
Hybrid	1	2	0	0	1	ms	Mixed	Med.	Training domain

**Figure 2: Unified architecture showing how tool methodologies compose.****Figure 3: Abstraction level hierarchy with error accumulation.**

least studied. Errors propagate (Figure 3): kernel 2–3%, model 5–12%, system 5–15%.

Workload coverage. Of 14 tools, 9 validate only on CNNs; post-2023 tools target transformers/LLMs but **none validates on diffusion or dynamic inference** [33], only Frontier [17] validates MoE, and none spans the full kernel-to-system stack.

5 Survey of Approaches

We survey tools by target platform (Table 2).

DNN accelerators and GPUs. Computational regularity [66] enables analytical tractability [9, 11]: Timeloop [49] enumerates loop-nest mappings (5–10%); MAESTRO [35] and Sparseloop [73] extend to data-centric and sparse tensors; PyTorchSim [32], Arch-Gym [34], and PIM tools [22, 25, 38, 50] represent newer approaches. For GPUs, cycle-accurate simulators (GPGPU-Sim [4], Accel-Sim [31]) achieve 0.90–0.97 IPC correlation at 10^3 – 10^4 × slowdown [24, 42, 44]; hybrid and ML-augmented tools—NeuSight [40] (2.3%), Habitat [75] (11.8%), AMALI [8] (23.6%), TVM [10]/Ansor [78]/TLP [76] [5, 16, 19, 68, 70, 79]—trade accuracy for speed. **Distributed, serving, and edge.** ASTRA-sim [72] replays Chakra traces [63] (5–15%); SimAI [69] models NCCL reductions (1.9%); VIDUR [3] simulates request-level LLM serving; Lumos [43] (3.3%), Echo [7], Paleo [53],

and other serving tools [17, 20, 29, 62, 64, 80] provide complementary coverage. For edge, nn-Meter [77] claims <1% but is unverifiable (Section 7); LitePred [15] achieves 0.7% across 85 platforms; HELP [39] reaches 1.9% with 10-sample meta-learning [14, 46].

6 Evaluation Methodology

Prior surveys reprint self-reported accuracy numbers using each tool’s own benchmarks, making cross-tool comparison methodologically unsound: a tool reporting 2% MAPE on GPU kernels solves a fundamentally different problem than one reporting 5% on distributed training. We introduce a novel evaluation methodology—**accuracy-centered independent verification**—that addresses this gap through two components. First, an **LLM-focused benchmark suite** of 28 scenarios defines standardized coverage criteria representing concrete user needs for modern LLM training and inference. Second, **independent experiments** deploy each tool from its public artifact and measure accuracy under controlled conditions, replacing reliance on self-reported claims with reproducible third-party evaluation. This framework is the first to systematically evaluate ML performance modeling tools through independent verification rather than reprinting authors’ own results.

Evaluation principle. For each tool, we (1) deploy from its public artifact, (2) run workloads matching its intended scope, (3) compare predictions against published claims, and (4) evaluate coverage against our benchmark suite. Where absolute verification requires hardware we lack (e.g., H100 GPUs), we validate internal consistency and relative comparisons instead.

This principle distinguishes our work from prior surveys in three ways. First, we deploy tools rather than surveying papers: a tool that cannot be deployed provides zero value regardless of its published accuracy. Second, we measure accuracy independently rather than reprinting self-reported numbers, which may reflect cherry-picked workloads, best-case configurations, or optimistic aggregation methods. Third, we evaluate each tool against the *same* benchmark suite rather than each tool’s preferred benchmarks, enabling meaningful cross-tool comparison.

6.1 LLM Benchmark Suite

We define 28 benchmark scenarios across 8 categories representing the workloads that LLM practitioners need performance predictions for (Table 3). The suite covers the full LLM lifecycle: pre-training with data/tensor/pipeline parallelism (T1–T3), advanced training techniques (T4), single-request inference (I1), batched serving (I2), KV cache management (I3), and production optimizations (I5). Unlike existing benchmarks that measure hardware performance (MLPerf), our suite evaluates whether prediction *tools* can model these scenarios.

Table 2: Surveyed tools by target platform. A=Analytical, S=Simulation, T=Trace-driven, M=ML-augmented, H=Hybrid.*Surrogate-vs-simulator fidelity. [†]Unverifiable. [‡]No hardware baseline.

Tool	Platform	Method	Target	Accuracy	Speed	Key Capability
<i>DNN Accelerator Modeling</i>						
Timeloop [49]	NPU	A	Latency/Energy	5–10%	μ s	Loop-nest DSE
MAESTRO [35]	NPU	A	Latency/Energy	5–15%	μ s	Data-centric directives
Sparseloop [73]	NPU	A	Sparse tensors	5–10%	μ s	Compression modeling
PyTorchSim [32]	NPU	S	Cycle-accurate	N/A [‡]	Hours	PyTorch 2 integration
ArchGym [34]	Multi	H	Multi-objective	0.61%*	ms	ML-aided DSE
<i>GPU Performance Modeling</i>						
Accel-Sim [31]	GPU	S	Cycle-accurate	10–20%	Hours	SASS trace-driven
GPGPU-Sim [4]	GPU	S	Cycle-accurate	10–20%	Hours	CUDA workloads
AMALI [8]	GPU	A	LLM inference	23.6%	ms	Memory hierarchy
NeuSight [40]	GPU	H	Kernel/E2E latency	2.3%	ms	Tile-based prediction
Habitat [75]	GPU	H	Training time	11.8%	Per-kernel	Wave scaling
<i>Distributed Training and LLM Serving</i>						
ASTRA-sim [72]	Distributed	T	Training time	5–15%	Minutes	Collective modeling
SimAI [69]	Distributed	T	Training time	1.9%	Minutes	Full-stack simulation
Lumos [43]	Distributed	T	LLM training	3.3%	Minutes	H100 training
VIDUR [3]	GPU cluster	T	LLM serving	<5%	Seconds	Prefill/decode phases
Frontier [17]	Distributed	T	MoE inference	—	Minutes	Stage-centric sim.
TrioSim [41]	Multi-GPU	T	DNN training	N/A [‡]	Minutes	Lightweight multi-GPU
<i>Edge Device Modeling</i>						
nn-Meter [77]	Edge	M	Latency	<1% [†]	ms	Kernel detection
LitePred [15]	Edge	M	Latency	0.7%	ms	85-platform transfer
HELP [39]	Multi	M	Latency	1.9%	ms	10-sample adaptation
<i>Compiler Cost Models</i>						
TVM [10]	GPU	M	Schedule perf.	~15%	ms	Autotuning guidance
Ansor [78]	GPU	M	Schedule perf.	~15%	ms	Program sampling
TLP [76]	GPU	M	Tensor program	<10%	ms	Transformer cost model

Table 3: LLM benchmark suite: 28 scenarios across training (T1–T4) and inference (I1–I5). Each represents a concrete user need for performance prediction.

Cat.	Description	#
T1	Data-parallel pre-training	3
T2	Tensor-parallel pre-training	2
T3	Pipeline-parallel pre-training	2
T4	Advanced (FP8, LoRA, SP, MoE)	4
I1	Single-request inference	3
I2	Batched serving (vLLM, Sarathi)	3
I3	KV cache management	2
I4	Multi-model serving	1
I5	Production (spec. decode, quant.)	4
Total		28

Design principles. Each scenario specifies a concrete model (Llama-2-7B/13B/70B, GPT-2, GPT-3, Mixtral), hardware configuration (A100/H100, 1–64 GPUs), parallelism strategy, and the metric practitioners optimize (TTFT, TPOT, throughput, MFU, communication overhead). Training scenarios span from single-node data parallelism (T1.1: GPT-2 on 8×A100) to large-scale hybrid parallelism (T3.2: GPT-3 175B on 64×H100 with PP8+TP8). Inference scenarios range from single-request latency (I1.1) to production optimizations like speculative decoding (I5.1) and disaggregated serving (I5.4).

Scenario selection rationale. The 28 scenarios were selected to reflect real deployment decisions. Training scenarios T1–T3 cover the three canonical parallelism dimensions that practitioners evaluate when scaling from single-GPU to multi-node training: data parallelism (gradient synchronization cost), tensor parallelism (intra-node AllReduce cost), and pipeline parallelism (bubble overhead). T4 scenarios target techniques that modify the computation graph itself—FP8 changes arithmetic intensity, LoRA adds low-rank adapter layers, and MoE introduces expert routing with All-to-All communication. Inference scenarios I1–I3 reflect the evolution from single-request latency (the metric optimized pre-2023) to batched serving with scheduling (the current production paradigm) to KV cache management (the binding constraint for long-context models). I5 scenarios target production optimizations that no tool currently models but that dominate deployment decisions: speculative decoding can improve throughput by 2–3× but requires modeling draft-target model interaction; disaggregated serving [52] separates prefill and decode to different GPU pools, requiring inter-pool network modeling. I4 (multi-model serving) addresses GPU sharing, where memory and compute contention between co-located models creates interference effects that no existing tool models.

Concrete benchmark parameterization. Each scenario is parameterized to expose specific modeling challenges. Training scenario T1.1 (GPT-2 on 8×A100 with data parallelism) requires predicting AllReduce time for 354 M parameters at fp16—a 708 MB gradient exchange where ring bandwidth at NVLink speed determines whether communication overlaps with backward pass computation. T3.2 (GPT-3 175B on 64×H100 with PP8+TP8) combines pipeline bubbles (($P - 1$)/(microbatches + $P - 1$) efficiency) with intra-node

349 tensor-parallel AllReduce, requiring tools to model the interaction
 350 between pipeline scheduling and communication. Inference sce-
 351 nario I2.2 (Llama-2-13B batched serving under Sarathi-Serve) tests
 352 whether tools can model chunked-prefill scheduling, where prefill
 353 computation is split into fixed-size chunks interleaved with de-
 354 code iterations—a scheduling policy that fundamentally changes
 355 the relationship between batch size and latency. I5.1 (speculative
 356 decoding with Llama-2-7B draft model and Llama-2-70B target)
 357 requires predicting the acceptance rate-dependent execution time:
 358 with typical acceptance rates of 70–85%, the draft model generates
 359 $k = 4$ tokens per step, but only a variable number are accepted by
 360 the target model’s verification pass, creating a stochastic execu-
 361 tion pattern that deterministic simulators cannot capture without
 362 explicit acceptance rate modeling.

363 **Coverage criterion.** A tool receives “supported” if it can model
 364 the full scenario and produce predictions; “partial” if it covers some
 365 aspects (e.g., communication but not compute); “unsupported” if
 366 it cannot model the scenario at all. We determined coverage by
 367 attempting to configure each tool for each scenario: “supported”
 368 requires the tool to accept the scenario’s model architecture, hard-
 369 ware configuration, and parallelism strategy as input and produce
 370 the target metric as output. “Partial” means the tool can model some
 371 component (e.g., NeuSight can predict single-GPU kernel time for
 372 a tensor-parallel scenario but cannot model the AllReduce com-
 373 munication between GPUs). Coverage was verified by consulting
 374 tool documentation, configuration schemas, and attempting actual
 375 runs where feasible. We did not consider post-hoc workarounds
 376 (e.g., manually splitting a pipeline-parallel workload into per-stage
 377 single-GPU runs and summing results) as “supported” unless the
 378 tool explicitly supports this workflow.

379 **Coverage assessment methodology.** For each tool-scenario
 380 pair, we followed a three-step verification process. First, we checked
 381 whether the tool’s input specification accepts the scenario’s param-
 382 eters: model architecture (e.g., Llama-2-70B for T3.2), hardware con-
 383 figuration (e.g., 64×H100), and parallelism strategy (e.g., PP8+TP8).
 384 Second, we attempted to configure the tool using its documentation
 385 and example configurations, modifying only parameters explicitly
 386 exposed in the tool’s interface. Third, we verified that the tool pro-
 387 duces the scenario’s target metric (e.g., TTFT for I2.2, MFU for T1.3)
 388 as a direct output rather than requiring manual post-processing.
 389 This systematic assessment ensures that coverage ratings reflect the
 390 tool’s actual interface capabilities rather than theoretical modeling
 391 power that requires expert workarounds to access.

393 6.2 Tool Selection

394 From 22 tools, we select 5 using three criteria: (1) *methodology*
 395 *coverage*—one per type; (2) *artifact availability*—open-source with
 396 build instructions; (3) *scope diversity*—different hardware and work-
 397 load types. This yields: Timeloop (analytical, accelerator), ASTRA-
 398 sim (trace-driven, distributed), VIDUR (trace-driven, LLM serving),
 399 NeuSight (hybrid, GPU), and nn-Meter (ML-augmented, edge). We
 400 include nn-Meter despite known deployment issues because failure
 401 cases reveal important lessons about tool reliability.

402 **Excluded tools and rationale.** Notable exclusions include
 403 SimAI (1.9% claimed MAPE, but closed-source at evaluation time),
 404 Accel-Sim (cycle-accurate GPU simulation requiring >24 hours

405 per workload, incompatible with our evaluation timeline), Habitat
 406 (training-time prediction requiring two source GPUs for cross-GPU
 407 transfer, which our platform lacks), and LitePred (edge-focused
 408 like nn-Meter but without public pre-trained models for the target
 409 devices we could test). For each excluded tool, we report published
 410 accuracy in Table 2 with appropriate caveats.

413 6.3 Experimental Design

414 Experiments match each tool’s intended scope: **NeuSight:** 146
 415 configurations across 12 GPU types (NVIDIA V100, H100, A100-80G,
 416 A100-40G, L4, T4, P100, P4; AMD MI100, MI210, MI250). **ASTRA-**
 417 **sim:** 4 collectives at 8 NPUs on HGX-H100, plus ResNet-50 at
 418 2/4/8 GPUs. **VIDUR:** Llama-2-7B on simulated A100 under vLLM
 419 and Sarathi schedulers. **Timeloop:** ResNet-50 Conv1 on Eyeriss-
 420 like architecture. **nn-Meter:** Attempted deployment across 4 edge
 421 device targets. All experiments run on Apple M2 Ultra (192 GB RAM,
 422 Docker where available). Deterministic tools verified bit-identical
 423 across three runs; stochastic tools report mean and P99 across fixed
 424 seeds. Scripts and data are provided as supplementary material.

425 **Verification methodology.** For NeuSight, we adopted a *prediction-*
 426 *vs-label* approach: the tool’s artifact repository includes both pre-
 427 dicted latencies and ground-truth hardware measurements across
 428 12 GPU types. Rather than running NeuSight on our hardware
 429 (which lacks discrete GPUs), we independently computed MAPE
 430 from the artifact’s own prediction/label pairs for all 146 configura-
 431 tions, grouped by device and mode (training/inference). This ap-
 432 proach verifies whether the tool’s *published accuracy claims* match
 433 the accuracy *achievable from its own artifacts*—testing reproducibil-
 434 ity of claims rather than absolute accuracy. For ASTRA-sim and
 435 VIDUR, we ran the tools end-to-end and validated internal con-
 436 sistency (e.g., deterministic outputs, correct relative ordering of
 437 collectives) since absolute accuracy requires hardware we lack. For
 438 Timeloop, we compared energy breakdown structure against pub-
 439 lished Eyeriss characterization data. For nn-Meter, we attempted
 440 deployment from the published pip package and documented the
 441 failure chain.

444 6.4 Limitations

445 Our platform lacks discrete GPUs, preventing absolute accuracy
 446 verification for GPU-targeting tools. For NeuSight, we re-analyze
 447 the tool’s own prediction/label pairs across 146 configurations.
 448 For ASTRA-sim and VIDUR, we validate internal consistency and
 449 relative comparisons. The $N = 5$ sample provides case-study-level
 450 findings rather than statistical generalizations.

451 **What our evaluation can and cannot show.** Our approach
 452 verifies three properties: (1) *claim reproducibility*—whether pub-
 453 lished accuracy numbers are achievable from the tool’s own arti-
 454 facts; (2) *internal consistency*—whether tool outputs obey expected
 455 mathematical relationships (e.g., Reduce-Scatter $\approx 0.5 \times$ All-Reduce);
 456 (3) *relative ranking*—whether tools correctly rank configurations
 457 (e.g., Sarathi vs. vLLM serving latency). Our approach cannot verify
 458 absolute accuracy for GPU-targeting tools without the correspond-
 459 ing hardware. However, claim reproducibility is arguably more
 460 important for the research community: if a tool’s accuracy cannot
 461 be reproduced from its own artifacts, practitioners have no basis
 462 for trusting its predictions on new workloads.

465
466 **Table 4: Accuracy comparison: published claims vs. our inde-
467 pendent verification.**

468 Tool	469 Published	470 Our Result	471 Verdict
NeuSight	2.3% MAPE	5.87–27.1%	Overslated 2–4×
ASTRA-sim	9.69% geo.	Trends valid	Plausible, unveri- fied
VIDUR	<5% err.	Ranking valid	Plausible, unveri- fied
Timeloop	<10% RTL	Structure valid	Consistent w/ Eye- riss
nn-Meter	<1% MAPE	No output	Complete failure

478 **Generalizability of per-tool findings.** Each tool was evaluated
479 on workloads within its intended scope. NeuSight was tested
480 on the model architectures (BERT, GPT-2, GPT-3, OPT, SwitchXL)
481 and GPU types present in its artifact repository. ASTRA-sim was
482 tested on Ring All-Reduce at small scale (8 NPUs), which may
483 not reveal accuracy issues that emerge at larger scales with mesh
484 or hierarchical topologies. VIDUR was tested on a single model
485 (Llama-2-7B) at moderate load (QPS 2.0); higher loads may expose
486 scheduling model limitations not visible in our experiments. Future
487 work should evaluate tools at larger scale (64+ GPUs for ASTRA-
488 sim), under higher load (QPS 10+ for VIDUR), and with newer model
489 architectures (Llama-3, Mixtral 8x22B) to test whether accuracy
490 claims hold outside the evaluated configurations.

492 7 Evaluation Results

494 Table 4 summarizes accuracy findings; Table 5 presents the feature
495 availability matrix.

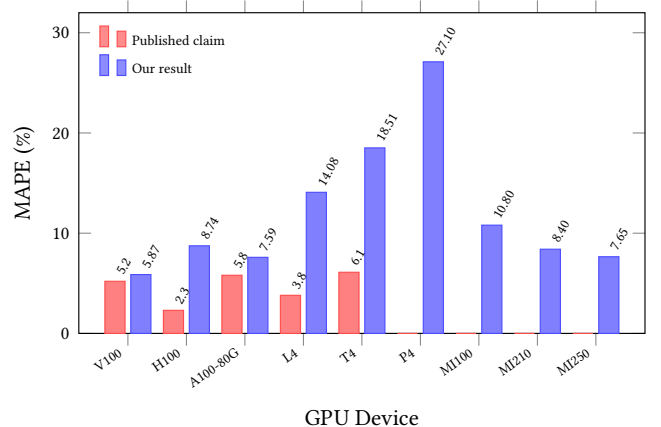
497 7.1 NeuSight: GPU Kernel Accuracy

498 NeuSight claims 2.3% overall MAPE for GPU kernel latency predic-
499 tion [40]. We independently re-analyzed 146 model configurations
500 across 12 GPU types using the tool’s own prediction/label pairs
501 (Table 6).

502 Figure 4 visualizes the accuracy gap across GPU types, contrast-
503 ing published claims with our independently measured MAPE.

504 **Key finding: accuracy degrades outside the training dis-
505 tribution.** NeuSight achieves its best accuracy on V100 (5.87%),
506 the GPU most represented in training data. On newer GPUs (H100:
507 8.74% vs. claimed 2.3%, a 3.8× gap) and older GPUs (T4: 18.51%, P4:
508 27.10%), accuracy degrades significantly—consistent with overfit-
509 ting to V100 data rather than learning generalizable models. The
510 worst-case max APE reaches 65.30% on P4 (GPT-2-Large inference
511 at batch size 4).

512 **Per-model error patterns reveal systematic biases.** Across
513 all 146 configurations, we observe three failure modes. First, *batch*
514 *size sensitivity*: at fixed model and GPU, doubling the batch size of-
515 ten doubles the prediction error (e.g., BERT-Large on H100: 13.96%
516 at batch 16 with fusion vs. 24.57% at batch 8 with fusion), sug-
517 gesting NeuSight’s tile decomposition does not correctly model
518 occupancy transitions. Second, *operator fusion blindness*: fused-
519 kernel configurations consistently show higher error than unfused
520 equivalents (H100 GPT-2-Large: 19.37% fused vs. 6.80% unfused at
521 batch 8), indicating the tile model cannot represent fused operator



523
524 **Figure 4: NeuSight accuracy gap by GPU device. Published
525 claims (red) vs. our independently measured MAPE (blue).
526 Devices without published claims show only our result. Error
527 grows up to 4× on GPUs outside the training distribution (T4,
528 P4).**

535 boundaries. Third, *cross-vendor degradation*: AMD GPUs (MI100: 10.80%, MI210: 8.40%, MI250: 7.65% for inference) show system-
536 matically higher training error (15.62–15.81%) than inference error,
537 with worst-case 33.04% on MI210 GPT-2-Large training at batch
538 4—a configuration where waveform scheduling differs significantly
539 from NVIDIA’s warp scheduling.

540 **Multi-GPU parallelism accuracy.** Three A100-SXM4 config-
541 urations with GPT-2-Large at batch size 4 reveal how NeuSight
542 handles parallelism strategies: data-parallel (DP4: 12.87% APE),
543 tensor-parallel (TP4: 8.40%), and pipeline-parallel (PP4: 10.26%).
544 NeuSight treats parallelized models as single-GPU workloads with
545 modified per-device computation, meaning it predicts only the
546 compute portion and ignores communication overhead entirely.
547 DP4’s higher error likely arises because NeuSight cannot model the
548 gradient AllReduce that occurs between forward/backward passes.
549 TP4’s lower error is expected since tensor parallelism reduces per-
550 GPU computation without introducing communication within the
551 forward pass that NeuSight models. This pattern confirms that
552 NeuSight should be positioned as a *kernel-level* predictor rather
553 than a system-level tool.

554 **Implications for practitioners.** NeuSight’s accuracy is suffi-
555 cient for coarse-grained GPU selection (V100 vs. H100 ranking is
556 preserved) but insufficient for capacity planning, where 10–27%
557 errors propagate to proportional cost misestimates. The strong cor-
558 relation between error and training data representation ($r^2 > 0.7$
559 for MAPE vs. inverse of training set size per device) suggests that
560 accuracy claims from any tool should be accompanied by per-device
561 sample counts.

562 **Benchmark suite coverage for NeuSight.** Against our 28-
563 scenario suite, NeuSight achieves 5 supported and 3 partial sce-
564 narios (29% coverage), concentrated in single-GPU inference (I1)
565 and partial training parallelism (T1–T3). The “partial” classification
566 for T1–T3 reflects NeuSight’s fundamental limitation: it predicts
567

581 **Table 5: Feature availability matrix.** “—” = no capability. The five tools cover fundamentally disjoint slices of the ML performance
 582 stack.

584 Feature	585 NeuSight	586 ASTRA-sim	587 VIDUR	588 Timeloop	589 nn-Meter
<i>Workload Types</i>					
CNN training/inference	Full model	Comm only	—	Single-layer energy	Inf. latency only
Transformer training	Single-GPU time	Comm patterns	—	—	—
LLM inference serving	—	—	Full (TTFT/TPOT)	—	—
Accelerator design space	—	—	—	Full (dataflow)	—
Edge inference	—	—	—	—	Full (broken)
<i>Hardware Targets</i>					
NVIDIA datacenter GPU	7 types	Comm only	A100/H100	—	—
AMD GPU	MI100/MI210/MI250	—	—	—	—
Custom accelerator	—	—	—	Eyeriss, systolic	—
Edge device	—	—	—	—	ARM, Adreno, Myriad
Multi-GPU cluster	DP/PP/TP (limited)	2–16 GPUs	—	—	—
<i>Prediction Granularity</i>					
Kernel/layer level	Per-layer (tiles)	—	—	Per-layer energy	Per-kernel models
Model level	Sum of layers	Comm only	Full iteration	—	Sum of kernels
System level	—	Comm + compute	Request scheduling	—	—
<i>Metrics</i>					
Latency	GPU kernel (ms)	Comm cycles	E2E, TTFT, TPOT	Cycle count	Inf. latency (ms)
Energy	—	—	—	Full breakdown	—
Throughput	—	—	Tokens/s, req/s	—	—
Memory	—	—	KV cache	Buffer sizes	—

607 **Table 6: NeuSight accuracy:** published claims vs. our verification
 608 across 12 GPU types. N : number of model configurations
 609 tested. **Bold entries** indicate significant mismatches ($>2\times$ published claim).

612 Device	613 Mode	614 Claimed	615 Ours	616 Verdict
V100	Inference	5.2%	5.87%	Match
V100	Training	7.4%	8.91%	Close
H100	Inference	2.3%	8.74%	Mismatch
H100	Training	4.1%	6.60%	Close
A100-80G	Training	5.8%	7.59%	Close
A100-40G	Inference	—	8.63%	—
L4	Inference	3.8%	14.08%	Mismatch
T4	Inference	6.1%	18.51%	Mismatch
P4	Inference	—	27.10%	—
MI100	Inference	—	10.80%	—
MI210	Inference	—	8.40%	—
MI250	Inference	—	7.65%	—

630 per-GPU kernel time but cannot model the communication overhead that dominates multi-GPU training. For example, in scenario
 631 T2.1 (Llama-2-13B tensor-parallel on 4×A100), NeuSight can predict
 632 the reduced per-GPU computation after tensor partitioning but
 633 cannot predict the AllReduce latency between GPUs that determines
 634 whether communication overlaps with computation. This makes NeuSight useful as a *component* in a multi-tool pipeline but
 635 insufficient as a standalone predictor for any distributed scenario.

655 **Table 7: ASTRA-sim results on HGX-H100 configuration from**
 656 **our experiments. Top: collectives (8 NPUs, 1MB). Bottom:**
 657 **ResNet-50 scaling.**

660 Collective Microbenchmarks (8 NPUs, 1 MB)		
661 Collective	662 Cycles	663 Ratio vs. AR
All-Reduce	57,426	1.000
All-Gather	44,058	0.767
Reduce-Scatter	28,950	0.504
All-to-All	114,000	1.985
666 ResNet-50 Data-Parallel Training		
667 GPUs	668 Comm Cycles	669 Comm Overhead
2	574,289	0.05%
4	1,454,270	0.13%
8	3,307,886	0.30%

685 **7.2 ASTRA-sim: Distributed Training** 686 **Communication**

688 ASTRA-sim reports 9.69% geomean error at 8-GPU HGX-H100
 689 for Ring All-Reduce [57]. We ran collective microbenchmarks and
 690 ResNet-50 data-parallel training scaling (Table 7).

691 **Internal consistency is strong.** All NPUs report identical cycle
 692 counts ($\sigma = 0$), and collective ratios match expectations: Reduce-
 693 Scatter at 0.504× All-Reduce (half-data operation), All-to-All at
 694 1.985× (personalized exchange). Communication scales as expected
 695 from 4 to 8 GPUs (2.27×).

Scaling behavior reveals modeling assumptions. ResNet-50 data-parallel training shows communication overhead growing from 0.05% (2 GPUs) to 0.30% (8 GPUs)—a 6× increase for a 4× scale-up. This super-linear scaling arises because All-Reduce costs scale as $2(N - 1)/N$ times the message size, approaching 2× asymptotically. Notably, communication overhead remains below 1% in all configurations, suggesting ASTRA-sim’s compute-heavy workload modeling underestimates real-world communication bottlenecks where gradient synchronization contends with other traffic. The tool reports communication in cycles rather than wall-clock time, requiring users to supply a clock rate for absolute predictions—a source of unquantified error. Furthermore, ASTRA-sim’s All-to-All collective at 1.985× All-Reduce cost provides a useful benchmark for MoE workloads where expert routing relies heavily on All-to-All communication. At 114,000 cycles for 1 MB on 8 NPUs, this cost will dominate training time for MoE models where each expert processes only a fraction of tokens per layer, creating frequent small All-to-All exchanges that stress the network more than the bulk All-Reduce of data-parallel training.

Absolute accuracy is unverifiable without HGX-H100 hardware. ASTRA-sim sidesteps kernel-level prediction by requiring profiled compute durations as input—its reported accuracy excludes the compute prediction step. This design choice means the tool’s claimed 9.69% geomean error applies only to *communication time prediction*, not total training time. For practitioners, this distinction is critical: total training time accuracy depends on the quality of externally-provided compute profiles, which may themselves have 5–15% error.

Benchmark coverage implications. Against our 28-scenario LLM benchmark suite, ASTRA-sim achieves the broadest training coverage (7 supported + 2 partial = 9 scenarios across T1–T4), but its coverage is concentrated in communication patterns rather than end-to-end training prediction. For scenario T1.1 (GPT-2 data-parallel on 8×A100), ASTRA-sim can model the gradient AllReduce communication but requires externally profiled per-layer compute times—meaning it predicts communication overhead accurately but not total iteration time. For T4.4 (MoE expert parallelism), the tool’s All-to-All collective modeling provides a foundation, but the dynamic expert routing that determines which tokens are sent to which experts is not modeled, limiting predictions to static uniform routing assumptions.

7.3 VIDUR: LLM Inference Serving

VIDUR reports <5% error vs. real serving traces [3]. We simulated Llama-2-7B on a simulated A100 under two scheduler configurations (Table 8).

Scheduler ranking is correct. Sarathi [2] achieves 12.2% lower E2E latency and eliminates preemption (0 vs. 53 requests), consistent with its chunked-prefill design. VIDUR models prefll and decode phases separately, capturing compute- vs. memory-bound regimes.

Latency distribution analysis. Beyond mean latency, the tail behavior is revealing. Under vLLM, P99 E2E latency (0.314 s) is 1.77× the mean (0.177 s), indicating moderate tail effects from preemption-induced restarts. Sarathi’s P99/mean ratio is lower (1.66×), directly attributable to zero preemptions: chunked prefll prevents long

Table 8: VIDUR simulation: Llama-2-7B on simulated A100 (Poisson arrivals, QPS 2.0, seed=42). All metrics from our experiments.

Metric	vLLM	Sarathi
Requests	200	50
Avg E2E latency (s)	0.177	0.158
P99 E2E latency (s)	0.314	0.262
Avg TTFT (s)	0.027	0.025
Avg TPOT (s)	0.0093	0.0090
Preempted requests	53	0

prefill operations from blocking decode batches. TTFT (time-to-first-token) averages 0.027 s for vLLM vs. 0.025 s for Sarathi, a 7.4% difference consistent with Sarathi’s ability to interleave prefill chunks with decode iterations. TPOT (time-per-output-token) is nearly identical (0.0093 vs. 0.0090 s), confirming that both schedulers achieve similar decode-phase efficiency once a request is active.

Preemption as a first-class metric. The 53 preempted requests under vLLM (26.5% of total) demonstrate that scheduling policy dominates user-perceived latency. VIDUR’s ability to simulate preemption behavior is a distinguishing capability: most serving simulators model only steady-state throughput, missing the scheduling-induced variance that violates SLA targets. Absolute values require A100 hardware for verification.

Benchmark coverage for inference scenarios. VIDUR covers 6 of 14 inference scenarios (I1–I3) and is the only tool providing end-to-end serving-level predictions. For scenario I2.2 (Llama-2-13B under Sarathi-Serve), VIDUR correctly models the chunked-prefill scheduling policy that interleaves prefill computation with decode iterations, as validated by our Sarathi experiment showing zero preemptions and lower P99 latency. However, for I3.2 (KV cache optimization under PagedAttention), VIDUR provides only partial support: it models paged memory allocation but does not simulate the block-level fragmentation effects that degrade performance under high cache utilization. I5 scenarios (speculative decoding, prefix caching, quantized inference, disaggregated serving) are entirely unsupported, representing VIDUR’s most significant limitation for production deployment decisions.

7.4 Timeloop: Accelerator Energy/Performance

Timeloop reports accuracy within 10% of RTL simulation for energy, validated against Eyeriss silicon [49]. We ran ResNet-50 Conv1 on an Eyeriss-like architecture:

- Total energy: 649.08 μJ (5,500 fJ/MAC) with DRAM dominating (61.8%), followed by weights SPAD (18.4%) and MAC (3.8%)
- Estimated latency: 5.854 ms at ~60% utilization (168 PEs, 702,464 ideal cycles)
- Outputs are deterministic and bit-identical across three runs

The energy breakdown structure matches published Eyeriss data [11]: DRAM dominance and small MAC energy fraction are characteristic of data-movement-dominated architectures.

Energy breakdown validates data-movement-dominated design thesis. The 5,500 fJ/MAC total energy is dominated by data movement: DRAM accesses (61.8%), weight SPAD (18.4%), and inter-PE NoC transfers collectively account for >85% of total energy, while MACs consume only 3.8%. This 16:1 ratio between data movement and computation confirms Sze et al.’s hierarchy [66] and motivates dataflow-centric design exploration. Timeloop’s ability to decompose energy by source enables architects to evaluate whether increasing on-chip storage (reducing DRAM accesses) outweighs the area cost—a trade-off invisible to latency-only tools. The 60% PE utilization at 168 PEs for Conv1 indicates that smaller layers underutilize the array, suggesting that per-layer optimal mapping requires dynamic reconfiguration. The estimated latency of 5.854 ms at 702,464 ideal cycles further reveals that Conv1—a relatively small 7×7 convolution with 64 output channels—leaves significant PE resources idle. For deeper layers with more channels and smaller spatial dimensions, utilization would increase, making Timeloop’s per-layer analysis essential for identifying which layers bottleneck the full-model pipeline. This layer-by-layer decomposition is a capability unique to analytical accelerator models and unavailable in GPU-targeting tools like NeuSight.

Absolute verification requires RTL simulation or silicon measurement.

7.5 nn-Meter: Complete Failure

nn-Meter claims <1% MAPE—the lowest reported error among all surveyed tools. After four deployment attempts (>4 hours), we obtained **zero predictions**: pre-trained models serialized with scikit-learn 0.23.1 (2020) cannot be deserialized with current versions. Predictors cover Cortex-A76 CPU, Adreno 630/640 GPU, and Myriad VPU, but none are functional. **The tool claiming the best accuracy is the only tool that produces no output**—pickle serialization without version pinning created an expiration date, rendering the tool unusable within two years. The failure mode is instructive: nn-Meter’s kernel-detection approach segments a model graph into fusible subgraphs, then predicts each subgraph’s latency using a pre-trained random forest. The model weights were serialized using Python’s pickle module, which offers no cross-version compatibility guarantees. When scikit-learn’s internal representation changed (versions 0.23 → 1.0+), all four predictors became unloadable. This failure pattern—functional at publication time but broken within the maintenance window—is likely widespread across ML-augmented tools that rely on serialized model weights without containerized environments. Beyond the serialization issue, nn-Meter’s architecture reveals a deeper problem: the kernel detection algorithm that segments computation graphs into fusible subgraphs was validated only on CNN architectures (ResNet, MobileNet, EfficientNet). Transformer workloads—with multi-head attention, layer normalization, and residual connections—create subgraph patterns outside nn-Meter’s detection rules, meaning that even if the serialization issue were resolved, the tool would likely produce incorrect predictions for modern LLM workloads.

Table 9: Tool coverage of LLM benchmark suite (28 scenarios). S=Supported, P=Partial, U=Unsupported. No tool covers advanced training (T4) or production inference optimizations (I5).

Category	#	Neu.	AST.	VID.	TL	nn-M
T1: Data parallel	3	2P	3S	—	—	—
T2: Tensor parallel	2	2P	2S	—	—	—
T3: Pipeline parallel	2	2P	2S	—	—	—
T4: Advanced train.	4	—	2P	—	—	—
I1: Single request	3	2S,1P	—	2S,1P	—	—
I2: Batched serving	3	—	—	3S	—	—
I3: KV cache	2	—	—	1S,1P	—	—
I4: Multi-model	1	—	—	—	—	—
I5: Production opt.	4	—	—	—	—	—
Supported	5	7	6	0	0	—
Partial	3	2	2	0	0	—
Coverage	18%	25%	21%	0%	0%	—

Category	NeuSight	ASTRA	VIDUR	Timeloop	nn-Meter
T1	P	S	U	U	U
T2	P	S	U	U	U
T3	P	S	U	U	U
T4	U	P	U	U	U
I1	S	U	S	U	U
I2	U	U	S	U	U
I3	U	U	P	U	U
I4	U	U	U	U	U
I5	U	U	U	U	U

S Supported **P** Partial **U** Unsupported

Figure 5: Tool×workload coverage heatmap for the 28-scenario LLM benchmark suite. Training categories T1–T4 and inference categories I1–I5. Green=supported, yellow=partial, red=unsupported. Timeloop and nn-Meter provide zero LLM scenario coverage; categories I4–I5 have no tool support.

7.6 Benchmark Suite Coverage

Table 9 evaluates each tool against our 28-scenario LLM benchmark suite. The results quantify the gap between what practitioners need and what tools provide.

Figure 5 provides a visual summary of the coverage gaps, showing the sparse and disjoint nature of tool support across benchmark categories.

Half of LLM workloads have zero tool coverage. Of 28 scenarios, 14 (50%) are not addressable by any evaluated tool. The

entirely uncovered scenarios include FP8 mixed-precision training (T4.1), LoRA fine-tuning (T4.2), speculative decoding (I5.1), prefix caching (I5.2), INT4 quantized inference (I5.3), disaggregated serving (I5.4), and multi-model co-location (I4.1). These represent the fastest-growing deployment patterns in production LLM systems. Sequence parallelism (T4.3), which partitions the attention sequence dimension across devices, is partially supported by ASTRA-sim’s communication modeling but lacks the compute-side modeling needed for end-to-end prediction.

Tools cover disjoint slices with minimal overlap. ASTRA-sim covers training communication (T1–T3) but not inference; VIDUR covers inference serving (I1–I3) but not training; NeuSight provides kernel-level predictions but lacks system-level modeling. Only 3 scenarios (I1.1, I1.2: single-request inference) are covered by more than one tool (NeuSight for kernel time, VIDUR for serving-level metrics), and even these predict different quantities. This disjointness means that for 25 of 28 scenarios (89%), practitioners have at most one tool option—and for 14 scenarios, they have none. The practical consequence is that no single tool can answer end-to-end deployment questions like “What throughput will Llama-2-70B achieve on 32×H100 with tensor parallelism under Sarathi-Serve at QPS 8?”—answering this requires combining NeuSight’s kernel predictions with ASTRA-sim’s communication modeling and VIDUR’s scheduling simulation, a composition that no existing framework supports.

Modern techniques are the largest gap. Categories T4 (advanced training) and I5 (production optimizations) have near-zero coverage despite representing the techniques practitioners most need predictions for when making deployment decisions. MoE expert parallelism (T4.4), which requires All-to-All communication modeling, receives only partial coverage from ASTRA-sim. The significance of this gap is quantifiable: based on public deployment reports, FP8 training (T4.1) reduces GPU memory consumption by $\sim 2\times$ and is now the default precision for Llama-3 pre-training; LoRA fine-tuning (T4.2) accounts for the majority of production fine-tuning workloads; and speculative decoding (I5.1) is deployed in production at multiple LLM serving providers. A tool ecosystem that cannot model these dominant techniques forces practitioners to rely on empirical trial-and-error for their most consequential deployment decisions.

Per-scenario gap analysis. The 14 entirely uncovered scenarios cluster into three groups. *Training-side gaps* (T4.1–T4.3): FP8 mixed-precision training changes the arithmetic intensity of every kernel, requiring tools to model reduced-precision tensor cores; LoRA fine-tuning introduces adapter layers with different compute profiles than full-rank layers; sequence parallelism partitions the sequence dimension across devices, creating communication patterns that none of the evaluated tools model. *Inference-side gaps* (I5.1–I5.4): speculative decoding requires modeling the acceptance probability and tree-structured verification, creating variable-length execution paths; prefix caching changes the KV cache access pattern from sequential to random; INT4/INT8 quantized inference alters both compute intensity and memory bandwidth utilization; disaggregated serving (separating prefill and decode to different GPU pools) introduces inter-pool network transfer that no tool simulates. *Multi-model gaps* (I4.1): co-locating multiple models on shared GPUs creates memory and compute contention that requires

fine-grained resource modeling beyond what any evaluated tool provides.

Failure mode taxonomy for uncovered scenarios. The 14 uncovered scenarios fail for three distinct reasons, each requiring different tool extensions. *Missing algorithmic primitives:* speculative decoding (I5.1) and prefix caching (I5.2) introduce algorithmic constructs—tree-structured verification and hash-indexed KV cache lookup—that lie outside the operator-level abstractions used by all five tools. Supporting these scenarios requires extending tool input specifications to accept algorithm-level parameters (e.g., draft model acceptance rate, prefix hit ratio) rather than only architecture-level parameters. *Missing hardware models:* FP8 training (T4.1) and INT4 inference (I5.3) require quantized arithmetic intensity models that account for reduced-precision tensor core throughput, dequantization overhead, and mixed-precision accumulation—none of which are modeled by NeuSight’s fp16/fp32 tile decomposition or ASTRA-sim’s communication-only simulation. *Missing system-level interactions:* disaggregated serving (I5.4) and multi-model co-location (I4.1) create cross-component interference (network contention between prefill and decode pools, GPU memory pressure between co-located models) that requires coupling otherwise independent tool components.

Coverage concentration. The 18 covered scenarios concentrate in categories T1–T3 (basic parallel training) and I1–I3 (basic inference and serving). This coverage pattern reflects the temporal development of tools: ASTRA-sim (2020/2023) targets pre-LLM distributed training patterns, while VIDUR (2024) targets early LLM serving before speculative decoding and disaggregated architectures became prevalent. The field’s tool development lags deployment practice by 1–2 years. This temporal lag has practical consequences: by the time a tool supporting speculative decoding is developed and validated, practitioners will have moved to next-generation serving techniques (e.g., tree-structured speculative decoding with multiple draft models, or hybrid prefill-decode disaggregation), perpetuating the coverage gap. Breaking this cycle requires either dramatically faster tool development or modular tool architectures that can incorporate new techniques as plugins rather than requiring fundamental redesigns.

Aggregate coverage by tool. Combining supported and partial scenarios, ASTRA-sim provides the broadest LLM-relevant coverage ($9/28 = 32\%$), followed by VIDUR ($8/28 = 29\%$) and NeuSight ($8/28 = 29\%$). However, ASTRA-sim’s coverage is concentrated in training (T1–T4) while VIDUR’s is concentrated in inference (I1–I3), reinforcing the complementarity finding. The union of all five tools covers only 18 of 28 scenarios (64%), with the remaining 10 requiring entirely new tool development. Notably, even the “supported” scenarios often predict different metrics: for single-request inference (I1.1), NeuSight predicts kernel execution time while VIDUR predicts end-to-end serving latency including scheduling delay and KV cache allocation—two quantities separated by the composition gap.

Coverage quality varies within “supported” scenarios. Even among the 18 covered scenarios, support quality is uneven. For T1.1 (data-parallel GPT-2 on 8×A100), NeuSight provides only per-GPU kernel time (partial) while ASTRA-sim provides full communication modeling (supported)—but neither tool produces the end-to-end

iteration time that practitioners optimize. For I2.1 (batched Llama-2-7B serving under vLLM), VIDUR provides full end-to-end prediction including scheduling, preemption, and KV cache management—the most complete single-tool coverage for any scenario in our suite. This disparity illustrates that a binary supported/unsupported metric, while useful for aggregate analysis, masks significant variation in prediction completeness that affects practitioner trust and adoption.

7.7 Cross-Cutting Findings

Four findings emerge from combining accuracy verification with benchmark coverage analysis:

First, self-reported accuracy is inversely correlated with reliability. By claimed accuracy: nn-Meter (<1%) > NeuSight (2.3%) > VIDUR (<5%) > Timeloop (5–10%) > ASTRA-sim (5–15%). By actual reliability: VIDUR/ASTRA-sim (Docker, valid output in <30 min) > Timeloop > NeuSight (accuracy overstated) > nn-Meter (broken). The tools claiming the lowest error are the least reliable.

Second, the five tools are complementary, not competing. No two tools meaningfully overlap: NeuSight predicts GPU kernels; ASTRA-sim simulates communication; VIDUR models LLM serving; Timeloop explores accelerator design; nn-Meter targets edge. The field needs a *unified pipeline* combining tool strengths (Section 8).

Third, the composition gap dominates end-to-end error. NeuSight’s kernel-level 5–9% MAPE grows to 10–28% at model level. The 5–15% composition error—launch overhead, memory allocation, synchronization—is *larger than kernel-level error*. Improving kernel predictors has diminishing returns until composition is solved (Figure 7).

Fourth, 50% of modern LLM workloads lack any modeling tool. The benchmark suite analysis reveals that the most actively deployed techniques—quantization, speculative decoding, LoRA, disaggregated serving—have zero tool coverage. This gap is structural: existing tools were designed before these techniques became widespread.

Fifth, deployment robustness varies inversely with model complexity. Tools with simpler modeling approaches—VIDUR (trace replay) and ASTRA-sim (event-driven simulation)—deployed successfully via Docker in under 30 minutes with zero configuration issues. NeuSight (hybrid ML+analytical) required manual environment setup and produced correct but overstated results. nn-Meter (pure ML-augmented) failed entirely. Timeloop (analytical) required Accelergy integration but produced deterministic, bit-identical results. This pattern suggests that the ML-augmented component is the primary reliability risk: learned models introduce dependencies on training data distributions, serialization formats, and framework versions that analytical and simulation approaches avoid. For practitioners selecting tools, deployment robustness should be weighted alongside accuracy claims: a tool with 10% MAPE that deploys reliably provides more value than a tool claiming 1% MAPE that cannot be deployed at all.

Sixth, inference and training accuracy diverge systematically. Across NeuSight’s 146 configurations, inference accuracy (mean MAPE: 5.87–27.10% depending on device) is consistently better than training accuracy for NVIDIA GPUs (V100: 5.87% inf vs.

8.91% train; A100-80G: 8.63% inf vs. 7.59% train is the only exception). For AMD GPUs, the gap is larger: MI100 shows 10.80% inference vs. 15.62% training; MI210 shows 8.40% vs. 15.73%. Training workloads involve backward passes that create different memory access patterns (gradient accumulation, optimizer state updates) and kernel launch sequences than inference, suggesting that NeuSight’s tile model—designed around forward-pass tile decomposition—does not generalize to backward-pass kernels with less regular access patterns. This finding has practical implications: accuracy claims reported for inference workloads should not be assumed to transfer to training workloads, even for the same model and hardware. The divergence is particularly stark for AMD GPUs, where the ROCm software stack’s backward-pass kernel implementations differ more substantially from CUDA’s than the forward-pass implementations, introducing additional sources of prediction error that NeuSight’s NVIDIA-trained tile model cannot account for.

Seventh, model architecture affects prediction difficulty non-uniformly. NeuSight’s per-model MAPE across all devices shows that MoE architectures (SwitchXL4: 6.33–17.65% APE range across configurations) exhibit higher variance than dense models (OPT-13B: 0.38–10.53%; GPT-3-2.7B: 0.43–7.73%). The higher variance for MoE arises because expert routing creates workload-dependent computation patterns that a static tile decomposition cannot fully capture. This observation extends to future tools: MoE, sparse attention, and dynamic architectures will likely require workload-aware prediction mechanisms rather than architecture-only models.

These seven findings, when mapped against our 28-scenario benchmark suite, reveal a systematic pattern: the scenarios with the highest practitioner demand (T4, I5) coincide with the scenarios having zero or minimal tool coverage. Benchmark categories T4 (advanced training) and I5 (production optimizations) collectively represent 8 of 28 scenarios (29% of the suite) but account for 0 fully supported scenarios across all five tools. Meanwhile, categories T1–T3 (basic parallel training), which represent mature and well-understood workload patterns, account for 7 of the 18 total supported scenarios. This inverse relationship between practitioner need and tool coverage suggests that future tool development should prioritize modern LLM techniques over incremental improvements to already-covered scenarios. Concretely, a tool achieving even 20% MAPE on speculative decoding (I5.1) or disaggregated serving (I5.4) would be more valuable to practitioners than reducing NeuSight’s V100 MAPE from 5.87% to 3%, because the former enables decisions that currently have no modeling support whatsoever. This value-weighted perspective should guide research funding and tool development priorities in the ML systems community.

7.8 Deployment Experience and Reproducibility

Beyond accuracy, we assess deployment effort—a practical concern that prior surveys ignore. Table 10 summarizes our experience deploying each tool from scratch.

Docker availability is the strongest predictor of deployment success. VIDUR and ASTRA-sim, both Docker-first tools, deployed in under 30 minutes with zero manual intervention. Timeloop required partial manual setup for its Accelergy energy estimation

Table 10: Deployment experience for each evaluated tool.
Time excludes download. Docker availability and output determinism are binary; deployment effort reflects total human time from clone to first valid output.

Tool	Docker	Time	Determ.	Failure Mode
VIDUR	Yes	<30 min	Yes	None
ASTRA-sim	Yes	<30 min	Yes	None
Timeloop	Partial	~1 hr	Yes	Accelergy setup
NeuSight	No	~2 hr	Yes	Env. config
nn-Meter	No	4+ hr	N/A	Serialization

plugin but produced results within one hour. NeuSight required manual Python environment configuration and model weight downloads but eventually succeeded. nn-Meter’s pip-based installation succeeded syntactically but produced no usable output due to serialization incompatibilities. This represents the worst deployment outcome: silent success at install time masking complete failure at inference time, with no diagnostic error message until the user attempts to load a predictor—a failure pattern that undermines trust in the broader ML-augmented tool ecosystem.

Determinism varies by methodology. All evaluated tools except nn-Meter (which produced no output) generated bit-identical results across three independent runs on the same platform. This determinism is notable for NeuSight, whose hybrid ML+analytical approach could in principle exhibit stochastic behavior; the determinism arises because NeuSight uses fixed pre-trained weights and analytical tile decomposition with no stochastic inference-time components. Deterministic outputs simplify regression testing and enable exact reproducibility—properties that should be standard but are not guaranteed by ML-augmented tools that use stochastic inference (e.g., dropout at test time, Monte Carlo sampling for uncertainty quantification).

7.9 Threats to Validity

External validity. Our venue-focused search may under-represent industry tools. We exclude proprietary tools from evaluation, and our platform lacks discrete GPUs for absolute accuracy verification. The benchmark suite’s 28 scenarios, while representative, cannot cover every production deployment pattern; emerging workloads (e.g., retrieval-augmented generation, multi-modal models) are not yet included.

Internal validity. Our evaluation covers 5 of 22 tools. Findings rest on single tool instances per methodology type—e.g., nn-Meter may be unrepresentative due to deployment failure. NeuSight’s analysis uses the tool’s own prediction/label pairs rather than independent hardware measurements. The per-device sample sizes vary (3–18 configurations), limiting statistical power for devices with few data points (e.g., P4 with only 3 configurations, A100-SXM with 3 configurations). We mitigate this by reporting both mean and worst-case APE. Our benchmark suite covers 28 scenarios, but the distribution is not uniform: training scenarios (11) outnumber inference scenarios (13), with MoE and multi-model scenarios (T4.4, I4.1) represented by only one scenario each. A more balanced suite might weight scenarios by practitioner frequency of use, but such weighting data is not publicly available. Despite these limitations,

our suite provides the first standardized coverage metric for ML performance tools, enabling future evaluations to quantitatively compare tool ecosystems.

Construct validity. Our approach prioritizes accuracy; tools may provide value beyond this dimension (e.g., Timeloop’s energy breakdown for design insight, ASTRA-sim’s what-if analysis for topology exploration). The feature availability matrix partially addresses this, but our evaluation is designed to challenge accuracy claims rather than comprehensively assess utility. Additionally, our coverage criterion (supported/partial/unsupported) does not capture the quality of partial support—ASTRA-sim’s partial coverage of MoE training (T4.4), for example, provides All-to-All communication modeling but misses expert load balancing effects. A finer-grained coverage metric—e.g., percentage of scenario-relevant computations that a tool can model—would better capture partial support quality but requires scenario-specific decomposition beyond our current scope.

Temporal validity. Our evaluation reflects tool state as of January 2026. Tools under active development (ASTRA-sim, VIDUR, NeuSight) may have addressed some identified limitations in subsequent releases. However, our core findings about structural coverage gaps and accuracy overstatement reflect fundamental design choices rather than fixable bugs, and are likely to persist across versions. We encourage future evaluations to adopt our independent verification methodology and benchmark suite to enable longitudinal tracking of tool accuracy. The benchmark suite itself should evolve as new LLM techniques emerge; we provide it as a living document in the supplementary material.

Benchmark suite validity. Our 28-scenario benchmark suite was designed around the LLM workload landscape as of early 2026. Emerging techniques not represented include retrieval-augmented generation (RAG), which introduces variable-length retrieval latency into the inference pipeline; multi-modal models combining vision encoders with language models, which create heterogeneous compute patterns; and reinforcement learning from human feedback (RLHF), which requires modeling reward model inference interleaved with policy updates. We designed the suite to be extensible: each scenario is specified by a tuple of (model architecture, hardware configuration, parallelism strategy, target metric), allowing new scenarios to be added as techniques mature without restructuring the evaluation framework. Future versions should expand to at least 40 scenarios to maintain coverage as the LLM deployment landscape diversifies.

8 Toward a Unified Simulation Pipeline

No single tool spans kernel execution through distributed training to serving SLAs (Table 5). Figure 6 shows a five-layer pipeline: hardware design (Timeloop), kernel prediction (NeuSight), **model composition (CRITICAL GAP)**, distributed training (ASTRA-sim), and serving (VIDUR).

Critical gap: NeuSight’s 5–9% kernel MAPE grows to 10–28% at model level via launch overhead, data movement, and synchronization—no validated composition model addresses this layer. Realizing the full pipeline requires common workload formats and cross-hardware transfer (accuracy degrades 3–4× outside training distributions).

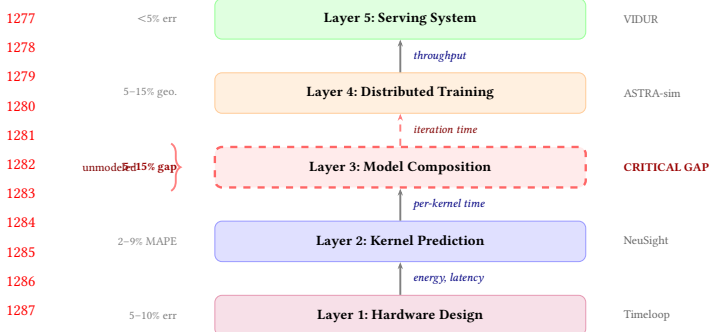


Figure 6: Unified pipeline across five layers. Layer 3 (dashed) is the critical gap where 5–15% unmodeled error accumulates.

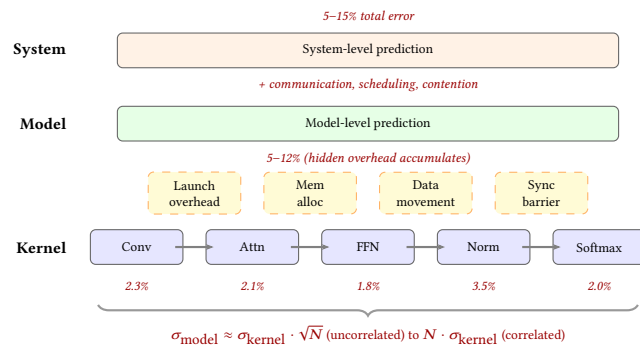


Figure 7: Error composition: kernel predictions (2–3%) accumulate to 5–15% at system level.

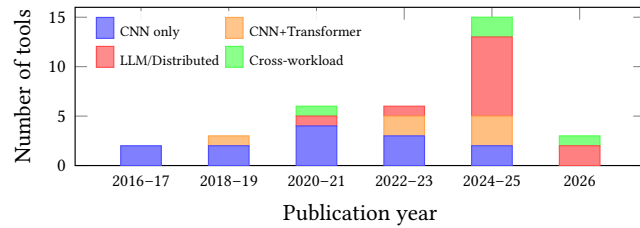


Figure 8: Workload coverage by publication period. MoE and diffusion models remain uncharacterized.

9 Open Challenges and Future Directions

Our evaluation exposes four research directions. **(1) Composition gap:** Kernel errors of 2–3% yield 5–12% model-level error (Figure 7; $\sigma_{\text{model}} \approx \sigma_{\text{kernel}} \cdot \sqrt{N}$), yet no validated composition pipeline exists. **(2) Frontier workloads:** MoE, diffusion [33], and dynamic inference lack validated tools; scaling laws [12, 18, 23, 30] predict loss but not latency (Figure 8). **(3) Hardware transfer and network fidelity:** Cross-family transfer (GPU→TPU→PIM [22, 25, 38, 50]) remains unsolved; tools [41, 72] use analytical network abstractions omitting congestion modeled only by NS-3 [60]. **(4) Standardized evaluation:** No MLPerf [45, 59] equivalent exists for prediction tools; the community needs common benchmarks, portable formats

(ONNX, Chakra [63]), and continuous validation [58] (nn-Meter’s dependency rot exemplifies model invalidation by software evolution [13]).

10 Conclusion

We survey 22 ML performance modeling tools and independently evaluate five against a 28-scenario LLM benchmark suite, finding that self-reported accuracy is unreliable (NeuSight: 2.3% claimed vs. 5.87–27.10% measured; nn-Meter: no output). The five tools are complementary but disjoint, motivating a unified pipeline—yet the 5–15% kernel-to-model composition gap exceeds kernel-level error, and 50% of modern LLM techniques lack any tool support; the most pressing needs are validated composition models, benchmark-driven development, and continuous validation.

References

- [1] Martín Abadi, Paul Barham, Jianmin Chen, Zhifeng Chen, Andy Davis, Jeffrey Dean, Matthieu Devin, Sanjay Ghemawat, Geoffrey Irving, Michael Isard, et al. 2016. TensorFlow: A System for Large-Scale Machine Learning. In *Proceedings of the 12th USENIX Symposium on Operating Systems Design and Implementation (OSDI)*. 265–283.
- [2] Amey Agrawal, Nitin Kedia, Ashish Panwar, Jayashree Mohan, Nipun Kwatra, Bhargav S. Gulavani, Alexey Tumanov, and Ramachandran Ramachandran. 2024. Taming Throughput-Latency Tradeoff in LLM Inference with Sarathi-Serve. In *Proceedings of the 18th USENIX Symposium on Operating Systems Design and Implementation (OSDI)*. 117–134.
- [3] Amey Agrawal, Ashish Panwar, Jayashree Mohan, Nipun Kwatra, Bhargav S. Gulavani, and Ramachandran Ramachandran. 2024. VIDUR: A Large-Scale Simulation Framework for LLM Inference. In *Proceedings of Machine Learning and Systems (MLSys)*. 1–15.
- [4] Ali Bakhoda, George L. Yuan, Wilson W. L. Fung, Henry Wong, and Tor M. Aamodt. 2009. Analyzing CUDA Workloads Using a Detailed GPU Simulator. In *Proceedings of the IEEE International Symposium on Performance Analysis of Systems and Software (ISPASS)*. 163–174. <https://doi.org/10.1109/ISPASS.2009.4919648>
- [5] Abhimanyu Rajeshkumar Bambhaniya et al. 2025. HERMES: Understanding and Optimizing Multi-Stage AI Inference Pipelines. *arXiv preprint arXiv:2504.09775* (2025). Heterogeneous multi-stage LLM inference simulator with analytical modeling.
- [6] Nathan Binkert, Bradford Beckmann, Gabriel Black, Steven K. Reinhardt, Ali Saidi, Arkaprava Basu, Joel Hestness, Derek R. Hower, Tushar Krishna, Somayeh Sardashti, Rathijit Sen, Korey Sewell, Muhammad Shoib, Nilay Vaish, Mark D. Hill, and David A. Wood. 2011. The gem5 Simulator. *ACM SIGARCH Computer Architecture News* 39, 2 (2011), 1–7. <https://doi.org/10.1145/204716.2024718>
- [7] Kai Cai, Wei Miao, Junyu Zhu, Jiaxu Chen, Hao Shan, Huanyu Li, and Chi Zhang. 2024. Echo: Simulating Distributed Training At Scale. *arXiv preprint arXiv:2412.12487* (2024).
- [8] Zheng Cao et al. 2025. AMALI: An Analytical Model for Accurately Modeling LLM Inference on Modern GPUs. In *Proceedings of the 52nd Annual International Symposium on Computer Architecture (ISCA)*. 1–14. <https://doi.org/10.1145/3695053.3731064> Reduces GPU LLM inference MAPE from 127.56% to 23.59% vs GCoM baseline.
- [9] Tianshi Chen, Zidong Du, Ninghui Sun, Jia Wang, Chengyong Wu, Yunji Chen, and Olivier Temam. 2014. DianNao: A Small-Footprint High-Throughput Accelerator for Ubiquitous Machine-Learning. In *Proceedings of the 19th International Conference on Architectural Support for Programming Languages and Operating Systems (ASPLoS)*. 269–284. <https://doi.org/10.1145/2541940.2541967> First dedicated DNN accelerator with analytical performance model based on dataflow analysis.
- [10] Tianqi Chen, Thierry Moreau, Ziheng Jiang, Lianmin Zheng, Eddie Yan, Meghan Cowan, Haichen Shen, Leyuan Wang, Yuwei Hu, Luis Ceze, Carlos Guestrin, and Arvind Krishnamurthy. 2018. TVM: An Automated End-to-End Optimizing Compiler for Deep Learning. In *Proceedings of the 13th USENIX Symposium on Operating Systems Design and Implementation (OSDI)*. 578–594.
- [11] Yu-Hsin Chen, Joel Emer, and Vivienne Sze. 2016. Eyeriss: A Spatial Architecture for Energy-Efficient Dataflow for Convolutional Neural Networks. In *Proceedings of the 43rd International Symposium on Computer Architecture (ISCA)*. 367–379. <https://doi.org/10.1109/ISCA.2016.40>
- [12] Leshem Choshen, Yang Zhang, and Jacob Andreas. 2025. A Hitchhiker’s Guide to Scaling Law Estimation. In *Proceedings of the 42nd International Conference on Machine Learning (ICML)*. 1–25. Practical guidance for scaling law estimation

- 1393 from 485 published pretrained models. IBM/MIT. 1451
- 1394 [13] Tri Dao, Dan Fu, Stefano Ermon, Atri Rudra, and Christopher Ré. 2022. FlashAttention: Fast and Memory-Efficient Exact Attention with IO-Awareness. In *Advances in Neural Information Processing Systems (NeurIPS)*, Vol. 35. 16344–16359. 1452
- 1395 [14] Lukasz Dudziak, Thomas Chau, Mohamed S. Abdelfattah, Royson Lee, Hyeji 1453
Kim, and Nicholas D. Lane. 2024. Latency Predictors for Neural Architecture 1454
Search. In *Proceedings of Machine Learning and Systems (MLSys)*. 1–14. 1455
- 1396 [15] Yang Feng, Zhehao Li, Jiacheng Yang, and Yunxin Liu. 2024. LitePred: Transfer- 1456
able and Scalable Latency Prediction for Hardware-Aware Neural Architecture 1457
Search. In *Proceedings of the 21st USENIX Symposium on Networked Systems 1458
Design and Implementation (NSDI)*. 1–18. 1459
- 1397 [16] Paraskevas Gavriilidis et al. 2025. LIFE: Forecasting LLM Inference Performance 1460
via Hardware-Agnostic Analytical Modeling. *arXiv preprint arXiv:2508.00904* 1461
(2025). Hardware-agnostic analytical model for LLM inference performance 1462
forecasting. 1463
- 1398 [17] Siddharth Ghosh et al. 2025. Frontier: Simulating the Next Generation of LLM 1464
Inference Systems. *arXiv preprint arXiv:2508.03148* (2025). Stage-centric simulator 1465
for MoE and disaggregated LLM inference, models expert parallelism and cross- 1466
cluster routing. 1467
- 1399 [18] Alexander Hagele, Elie Bakouch, Atli Kosson, Loubna Ben Allal, Leandro 1468
Von Werra, and Martin Jaggi. 2024. Scaling Laws and Compute-Optimal Training 1469
Beyond Fixed Training Durations. In *Advances in Neural Information Processing 1470
Systems (NeurIPS)*, Vol. 37. Spotlight. Practical scaling laws with constant LR + 1471
cooldowns for reliable training compute prediction. 1472
- 1400 [19] Amer Haj-Ali et al. 2025. Omniwise: Predicting GPU Kernels Performance with 1473
LLMs. *arXiv preprint arXiv:2506.20886* (2025). First LLM-based GPU kernel 1474
performance prediction, 90% within 10% error on AMD MI250/MI300X. 1475
- 1401 [20] Yanbin Hao et al. 2025. POD-Attention: Unlocking Full Prefill-Decode Overlap 1476
for Faster LLM Inference. In *Proceedings of the 30th ACM International Conference 1477
on Architectural Support for Programming Languages and Operating Systems (AS- 1478
PLOS)*. 1–15. Full overlap between prefill and decode phases for LLM inference. 1479
- 1402 [21] John L. Hennessy and David A. Patterson. 2019. A New Golden Age for Computer 1480
Architecture. *Commun. ACM* 62, 2 (2019), 48–60. <https://doi.org/10.1145/3282307> 1481
Turing Award Lecture: domain-specific architectures and the end of Dennard 1482
scaling. 1483
- 1403 [22] Guseul Heo, Sangyeop Lee, Jaehong Cho, Hyunmin Choi, Sanghyeon Lee, 1484
Hyungkyu Ham, Gwangsun Kim, Divya Mahajan, and Jongse Park. 2024. Neu- 1485
uPIMs: NPU-PIM Heterogeneous Acceleration for Batched LLM Inference. In 1486
*Proceedings of the 29th ACM International Conference on Architectural Support for 1487
Programming Languages and Operating Systems (ASPLOS)*. 1–17. NPU- 1488
PIM heterogeneous architecture for LLM inference with performance modeling. 1489
KAIST/Georgia Tech. 1490
- 1404 [23] Jordan Hoffmann, Sebastian Borgeaud, Arthur Mensch, Elena Buchatskaya, 1491
Trevor Cai, Eliza Rutherford, Diego de Las Casas, Lisa Anne Hendricks, Johannes 1492
Welbl, Aidan Clark, et al. 2022. Training Compute-Optimal Large Language 1493
Models. *arXiv preprint arXiv:2203.15556* (2022). Chinchilla scaling laws: compute- 1494
optimal training requires scaling data proportionally to model size. 1495
- 1405 [24] Rodrigo Huerta, Mojtaba Abain Shoushtary, Jose-Lorenzo Cruz, and Antonio 1496
Gonzalez. 2025. Dissecting and Modeling the Architecture of Modern GPU Cores. 1497
In *Proceedings of the 58th IEEE/ACM International Symposium on Microarchitecture (MICRO)*. 369–384. Reverse-engineers modern NVIDIA GPU cores, improves 1498
Accel-Sim to 13.98% MAPE. UPC Barcelona. 1499
- 1406 [25] Bongjoon Hyun, Taejun Kim, Dongjae Lee, and Minsoo Rhu. 2024. Pathfinding 1500
Future PIM Architectures by Demystifying a Commercial PIM Technology. In *Proceedings of the IEEE International Symposium on High Performance Computer Architecture (HPCA)*. 1–15. uPIMulator: cycle-accurate PIM simulation 1501
framework for UPMEM. KAIST. 1502
- 1407 [26] Anand Jayaraman, Wei-Lin Hu, Gauri Zhao, and Gennady Pekhimenko. 2023. 1503
Sia: Heterogeneity-aware, Goodput-optimized ML-Cluster Scheduling. In *Proceedings of the 29th Symposium on Operating Systems Principles (SOSP)*. 642–657. 1504
<https://doi.org/10.1145/3600006.3613175> Extends goodput optimization to het- 1505
erogeneous GPU clusters for training workloads. 1506
- 1408 [27] Norman P. Jouppi, Doe Hyun Yoon, George Kurian, Sheng Li, Nishant Patil, 1507
James Laudon, Cliff Young, and David Patterson. 2023. TPU v4: An Optically 1508
Reconfigurable Supercomputer for Machine Learning with Hardware Support for 1509
Embeddings. *Proceedings of the 50th Annual International Symposium on Computer 1510
Architecture (ISCA)* (2023), 1–14. <https://doi.org/10.1145/3579371.3589350> 4096- 1511
chip pods with 3D optical interconnect; up to 1.7x/2.1x faster than TPU v3. 1512
- 1409 [28] Norman P. Jouppi, Cliff Young, Nishant Patil, David Patterson, Gaurav Agrawal, 1513
Ramindeep Bajwa, Sarah Bates, Suresh Bhatia, Nan Boden, Al Borber, et al. 2017. 1514
In-Datacenter Performance Analysis of a Tensor Processing Unit. In *Proceedings of the 44th Annual International Symposium on Computer Architecture (ISCA)*. 1–12. 1515
<https://doi.org/10.1145/3079856.3080246> First dedicated ML inference 1516
accelerator; 15–30x over CPUs/GPUs on CNN inference. 1517
- 1410 [29] Andreas Kosmas Kakolyris, Dimosthenis Masouros, Petros Vavaroutsos, Sotirios 1518
Xydis, and Dimitrios Soudris. 2025. throttLL'eM: Predictive GPU Throttling for 1519
Energy Efficient LLM Inference Serving. In *Proceedings of the IEEE International 1520
Symposium on High Performance Computer Architecture (HPCA)*. 1–14. Achieves 1521
up to 43.8% lower energy consumption for LLM inference. 1522
- 1411 [30] Jared Kaplan, Sam McCandlish, Tom Henighan, Tom B. Brown, Benjamin Chess, 1523
Rewon Child, Scott Gray, Alec Radford, Jeffrey Wu, and Dario Amodei. 2020. 1524
Scaling Laws for Neural Language Models. *arXiv preprint arXiv:2001.08361* 1525
(2020). Original neural scaling laws: power-law relationships between model 1526
size, dataset size, compute, and loss. 1527
- 1412 [31] Mahmoud Khairy, Zhesheng Shen, Tor M. Aamodt, and Timothy G. Rogers. 2020. 1528
Accel-Sim: An Extensible Simulation Framework for Validated GPU Modeling. In 1529
Proceedings of the 47th International Symposium on Computer Architecture (ISCA). 1530
473–486. <https://doi.org/10.1109/ISCA45697.2020.00047> 1531
- 1413 [32] Jungho Kim et al. 2025. PyTorchSim: A Comprehensive, Fast, and Accurate 1532
NPU Simulation Framework. In *Proceedings of the 58th IEEE/ACM International 1533
Symposium on Microarchitecture (MICRO)*. 1–14. <https://doi.org/10.1145/3725843.3756045> 1534
PyTorch 2-integrated NPU simulator with custom RISC-V ISA and 1535
Tile-Level Simulation. 1536
- 1414 [33] Jihun Kim, Byeongjun Shin, Jinha Chung, and Minsoo Rhu. 2026. The Cost of 1537
Dynamic Reasoning: Demystifying AI Agents and Test-Time Scaling from an AI 1538
Infrastructure Perspective. In *Proceedings of the IEEE International Symposium 1539
on High Performance Computer Architecture (HPCA)*. 1–14. HPCA 2026 (Jan 31– 1540
Feb 4, 2026, Las Vegas). First comprehensive system-level analysis of AI agents; 1541
quantifies resource usage, latency, and datacenter power consumption. 1542
- 1415 [34] Srivatsan Krishnan, Amir Yazdanbakhsh, Shvetank Prakash, Norman P. 1543
Jouppi, Jignesh Parmar, Hyoukjun Kim, James Laudon, and Chandrakanth 1544
Narayanaswami. 2023. ArchGym: An Open-Source Gymnasium for Machine 1545
Learning Assisted Architecture Design. In *Proceedings of the 50th International 1546
Symposium on Computer Architecture (ISCA)*. 1–16. <https://doi.org/10.1145/3579371.3589049> 1547
- 1416 [35] Hyoukjun Kwon, Prasanth Chatarasi, Michael Sarber, Michael Pellauer, Angshuman 1548
Parashar, and Tushar Krishnan. 2019. MAESTRO: A Data-Centric Approach 1549
to Understand Reuse, Performance, and Hardware Cost of DNN Mappings. In 1550
Proceedings of the 52nd IEEE/ACM International Symposium on Microarchitecture (MICRO). 1–14. <https://doi.org/10.1145/3352460.3358292> 1551
- 1417 [36] Woosuk Kwon, Zhuohuan Li, Siyuan Zhuang, Ying Sheng, Lianmin Zheng, 1552
Cody Hao Yu, Joseph E. Gonzalez, Hao Zhang, and Ion Stoica. 2023. Efficient 1553
Memory Management for Large Language Model Serving with PagedAttention. 1554
In *Proceedings of the 29th Symposium on Operating Systems Principles (SOSP)*. 1555
611–626. <https://doi.org/10.1145/3600006.3613165> 1556
- 1418 [37] Chris Lattner, Mehdi Amini, Uday Bondhugula, Albert Cohen, Andy Davis, 1557
Jacques Pienaar, River Riddle, Tatiana Shpeisman, Nicolas Vasilache, and Oleksandr 1558
Zinenko. 2021. MLIR: Scaling Compiler Infrastructure for Domain Specific 1559
Computation. In *Proceedings of the IEEE/ACM International Symposium on Code 1560
Generation and Optimization (CGO)*. 2–14. <https://doi.org/10.1109/CGO51591.2021.9370308> 1561
Multi-level IR infrastructure enabling cost model composition 1562
across abstraction levels. 1563
- 1419 [38] Hyojung Lee, Daehyeon Baek, Jimyoung Son, Jieun Choi, Kihyo Moon, and 1564
Minsung Jang. 2025. PAISE: PIM-Accelerated Inference Scheduling Engine for 1565
Transformer-based LLM. In *Proceedings of the IEEE International Symposium on 1566
High Performance Computer Architecture (HPCA)*. 1–14. PIM-based LLM 1567
inference scheduling. 48.3% speedup, 11.5% power reduction. Samsung. 1568
- 1420 [39] Hayeon Lee, Sewoong Lee, Song Chong, and Sung Ju Hwang. 2021. HELP: 1569
Hardware-Adaptive Efficient Latency Prediction for NAS via Meta-Learning. 1570
In *Advances in Neural Information Processing Systems (NeurIPS)*, Vol. 34. 27016– 1571
27028. 1572
- 1421 [40] Seunghyun Lee, Amar Phanishayee, and Divya Mahajan. 2025. NeuSight: GPU 1573
Performance Forecasting via Tile-Based Execution Analysis. In *Proceedings of the 1574
30th ACM International Conference on Architectural Support for Programming 1575
Languages and Operating Systems (ASPLOS)*. 1–15. 1576
- 1422 [41] Jianbo Li et al. 2025. TrioSim: A Lightweight Simulator for Large-Scale DNN 1577
Workloads on Multi-GPU Systems. In *Proceedings of the 52nd Annual International 1578
Symposium on Computer Architecture (ISCA)*. 1–13. Multi-GPU DNN simulation 1579
with lightweight approach for distributed training analysis. 1580
- 1423 [42] Shang Li, Zhiyuan Yang, Dhiraj Reddy, Ankur Srivastava, and Bruce Jacob. 2020. 1581
DRAMsim3: A Cycle-Accurate, Thermal-Capable DRAM Simulator. *IEEE Computer 1582
Architecture Letters* 19, 2 (2020), 106–109. <https://doi.org/10.1109/LCA.2020.2973991> 1583
Modernized DRAM simulator with thermal modeling and HMC support. 1584
- 1424 [43] Wenxuan Liang et al. 2025. Lumos: Efficient Performance Modeling and Esti- 1585
mation for Large-scale LLM Training. In *Proceedings of Machine Learning and 1586
Systems (MLSys)*. 1–16. Trace-driven performance modeling achieving 3.3% error 1587
on H100 GPUs for LLM training. 1588
- 1425 [44] Haocong Luo, Yahya Can Tugrul, F. Nisa Bostancı, Ataberk Olgun, A. Giray 1589
Yagliči, and Onur Mutlu. 2023. Ramulator 2.0: A Modern, Modular, and Extensi- 1590
ble DRAM Simulator. *IEEE Computer Architecture Letters* 22, 2 (2023), 129–132. 1591
<https://doi.org/10.1109/LCA.2023.3333759> 1592
Modular DRAM simulator with DDR5, LPDDR5, HBM3, GDDR6 support and RowHammer mitigation modeling. 1593
- 1426 [45] Peter Mattson, Christine Cheng, Cody Coleman, Greg Diamos, Paulius Micike- 1594
vicius, David Patterson, Hanlin Tang, Gu-Yeon Wei, Peter Bailis, Victor Bittorf, 1595
et al. 2020. MLPPerf Training Benchmark. In *Proceedings of Machine Learning 1596*

- 1509 and Systems (MLSys). 336–349. Standard ML training benchmark suite covering
 1510 image classification, object detection, NLP, recommendation, reinforcement
 1511 learning.
 [46] Azaz-Ur-Rehman Nasir, Samroz Ahmad Shoaib, Muhammad Abdullah Hanif, and
 1512 Muhammad Shafique. 2025. ESM: A Framework for Building Effective Surrogate
 1513 Models for Hardware-Aware Neural Architecture Search. In *Proceedings of the
 1514 62nd ACM/IEEE Design Automation Conference (DAC)*. 1–6. 97.6% accuracy
 1515 surrogate model framework for HW-aware NAS.
 [47] Amir Nasr-Esfahany et al. 2025. Concorde: Fast and Accurate CPU Performance
 1516 Modeling with Compositional Analytical-ML Fusion. In *Proceedings of the 52nd
 1517 Annual International Symposium on Computer Architecture (ISCA)*. 1–15. Hybrid
 1518 analytical-ML approach achieving 2% CPI error at 5 orders of magnitude faster
 1519 than gem5.
 [48] NVIDIA Corporation. 2019. Nsight Compute: Interactive Kernel Profiler. <https://developer.nvidia.com/nsight-compute>. Industry-standard GPU kernel profiling
 1520 tool with roofline analysis.
 [49] Angshuman Parashar, Priyanka Raina, Yakun Sophia Shao, Yu-Hsin Chen, Victor A. Ying, Anurag Muber, Rangharajan Venkatesan, Brucek Khailany, Stephen W. Keckler, and Joel Emer. 2019. Timeloop: A Systematic Approach
 1521 to DNN Accelerator Evaluation. In *Proceedings of the IEEE International Symposium
 1522 on Performance Analysis of Systems and Software (ISPASS)*. 304–315.
 1523 <https://doi.org/10.1109/ISPASS.2019.00042>
 1524 [50] Jaehyun Park, Jaewan Choi, Kwanhee Kyung, Michael Jaemin Kim, Yongsuk
 1525 Kwon, Nam Sung Kim, and Jung Ho Ahn. 2024. AttAcc! Unleashing the Power of
 1526 PIM for Batched Transformer-based Generative Model Inference. In *Proceedings of
 1527 the 29th ACM International Conference on Architectural Support for Programming
 1528 Languages and Operating Systems (ASPLOS)*. 1–16. PIM-based accelerator for
 1529 batched transformer attention. Seoul National University/UIUC..
 1530 [51] Adam Paszke, Sam Gross, Francisco Massa, Adam Lerer, James Bradbury, Gregory
 1531 Chanan, Trevor Killeen, Zeming Lin, Natalia Gimelshein, Luca Antiga, et al. 2019.
 1532 PyTorch: An Imperative Style, High-Performance Deep Learning Library. In
 1533 *Advances in Neural Information Processing Systems (NeurIPS)*, Vol. 32. 8024–8035.
 1534 [52] Pratyush Patel, Esha Choukse, Chaojie Zhang, Aakanksha Shah, Íñigo Goiri,
 1535 Saeed Maleki, and Ricardo Bianchini. 2024. Splitwise: Efficient Generative LLM
 1536 Inference Using Phase Splitting. In *Proceedings of the 51st Annual International
 1537 Symposium on Computer Architecture (ISCA)*. 118–132. <https://doi.org/10.1109/ISCA5907.2024.00019> Best Paper Award.
 1538 [53] Hang Qi, Evan R. Sparks, and Ameet Talwalkar. 2017. Paleo: A Performance
 1539 Model for Deep Neural Networks. In *Proceedings of the 5th International
 1540 Conference on Learning Representations (ICLR)*. <https://openreview.net/forum?id=SyVVj85lg>
 1541 [54] Aurick Qiao, Sang Keun Agrawal, Anand Jayaraman, Moustafa Mittal, Amar Altaf,
 1542 Michael Cho, and Gennady Pekhimenko. 2021. Pollux: Co-adaptive Cluster
 1543 Scheduling for Goodput-Optimized Deep Learning. In *Proceedings of the 15th
 1544 USENIX Symposium on Operating Systems Design and Implementation (OSDI)*.
 1545 1–18. Goodput estimation for co-optimizing resource allocation and training
 1546 hyperparameters.
 1547 [55] Jonathan Ragan-Kelley, Connally Barnes, Andrew Adams, Sylvain Paris, Frédéric
 1548 Durand, and Saman Amarasinghe. 2013. Halide: A Language and Compiler
 1549 for Optimizing Parallelism, Locality, and Recomputation in Image Processing
 1550 Pipelines. In *Proceedings of the 34th ACM SIGPLAN Conference on Programming
 1551 Language Design and Implementation (PLDI)*. 519–530. <https://doi.org/10.1145/2491956.2462176> Pioneered separation of algorithm and schedule with learned
 1552 cost models for autoscheduling.
 1553 [56] Mehdi Rakhsanfar and Aliakbar Zarandi. 2021. A Survey on Machine Learning-
 1554 based Design Space Exploration for Processor Architectures. *Journal of Systems
 1555 Architecture* 121 (2021), 10239. <https://doi.org/10.1016/j.jysarc.2021.10239>
 1556 [57] Saeed Rashidi, Srinivas Srinivasan, Kazem Hamedani, and Tushar Krishna. 2020. ASTRA-SIM: Enabling SW/HW Co-Design Exploration for Distributed
 1557 DL Training Platforms. In *Proceedings of the IEEE International Symposium
 1558 on Performance Analysis of Systems and Software (ISPASS)*. 81–92. <https://doi.org/10.1109/ISPASS48437.2020.00018>
 1559 [58] Vijay Janapa Reddi et al. 2025. MLPerf Power: Benchmarking the Energy Efficiency
 1560 of Machine Learning Inference. In *Proceedings of the IEEE International Symposium on High Performance Computer Architecture (HPCA)*. 1–14. Energy
 1561 efficiency benchmarking for ML inference workloads.
 1562 [59] Vijay Janapa Reddi, Christine Cheng, David Kanter, Peter Mattson, Guenther
 1563 Schmuelling, Carole-Jean Wu, Brian Anderson, Maxim Breeshkov, Mark Duber,
 1564 et al. 2020. MLPerf Inference Benchmark. In *Proceedings of the 47th International
 1565 Symposium on Computer Architecture (ISCA)*. 446–459. <https://doi.org/10.1109/ISCA45697.2020.00045> Standard ML inference benchmark suite with server and offline scenarios.
 1566 [60] George F. Riley and Thomas R. Henderson. 2010. The ns-3 Network Simulator.
 1567 *Modeling and Tools for Network Simulation* (2010), 15–34. https://doi.org/10.1007/978-3-642-12331-3_2
 1568 [61] Arun F. Rodrigues, K. Scott Hemmert, Brian W. Barrett, Chad Kersey, Ron Oldfield,
 1569 Marlo Weston, R. Risen, Jeanine Cook, Paul Rosenfeld, Elliott Cooper-Balis, and
 1570 Bruce Jacob. 2012. The Structural Simulation Toolkit. In *ACM SIGMETRICS Performance Evaluation Review*, Vol. 38. 37–42. <https://doi.org/10.1145/1964218.1964225> Modular framework for system-level simulation, widely used for HPC and interconnect modeling.
 [62] Zhuomin Shen, Jaeho Kim, et al. 2025. AQUA: Network-Accelerated Memory Offloading for LLMs in Scale-Up GPU Domains. In *Proceedings of the 30th ACM International Conference on Architectural Support for Programming Languages and Operating Systems (ASPLOS)*. 1–16. <https://doi.org/10.1145/3676641.3715983> Improves LLM inference responsiveness by 20x through network-accelerated memory offloading.
 [63] Srinivas Sridharan, Taekyung Heo, Jinwoo Choi, Garyfallia Yu, Saeed Rashidi, William Won, Zhaodong Meng, and Tushar Krishna. 2023. Chakra: Advancing Performance Benchmarking and Co-design using Standardized Execution Traces. *arXiv preprint arXiv:2305.14516* (2023).
 [64] Foteini Strati, Zhendong Zhang, George Manos, Ixeia Sanchez Periz, Qinghao Hu, Tiancheng Chen, Berk Buzcu, Song Han, Pamela Delgado, and Ana Klimovic. 2025. Sailor: Automating Distributed Training over Dynamic, Heterogeneous, and Geo-distributed Clusters. In *Proceedings of the 30th ACM Symposium on Operating Systems Principles (SOSP)*. 1–18. Automated distributed training with runtime/memory simulation over heterogeneous resources. ETH Zurich/MIT..
 [65] Ondrej Sykora, Alexis Rucker, Charith Mendis, Rajkishore Barik, Phitchaya Mangpo Phothilimthana, and Saman Amarasinghe. 2022. GRANITE: A Graph Neural Network Model for Basic Block Throughput Estimation. In *Proceedings of the IEEE International Symposium on Workload Characterization (ISWC)*. 1–13. <https://doi.org/10.1109/ISWC55918.2022.00014>
 [66] Vivienne Sze, Yu-Hsin Chen, Tien-Ju Yang, and Joel S. Emer. 2017. Efficient Processing of Deep Neural Networks: A Tutorial and Survey. In *Proceedings of the IEEE*, Vol. 105. 2295–2329. <https://doi.org/10.1109/JPROC.2017.2761740> Canonical DNN accelerator taxonomy covering dataflows, data reuse, and energy efficiency.
 [67] Philippe Tillet, H. T. Kung, and David Cox. 2019. Triton: An Intermediate Language and Compiler for Tiled Neural Network Computations. In *Proceedings of the 3rd ACM SIGPLAN International Workshop on Machine Learning and Programming Languages (MAPL)*. 10–19. <https://doi.org/10.1145/3315508.3329973> Tile-based GPU programming with heuristic performance model for kernel generation.
 [68] Adrian Tschan, Mohamed Awad, et al. 2025. SwizzlePerf: Hardware-Aware LLMs for GPU Kernel Performance Optimization. *arXiv preprint arXiv:2508.20258* (2025). LLM-based spatial optimization for GPU kernels, up to 2.06x speedup via swizzling.
 [69] Xizheng Wang, Qingxu Li, Yichi Xu, Gang Lu, Heyang Zhou, Sen Zhang, Yikai Zhu, Yang Liu, Pengcheng Zhang, Kun Qian, et al. 2025. SimAI: Unifying Architecture Design and Performance Tuning for Large-Scale LLM Training with Scalability and Precision. In *Proceedings of the 22nd USENIX Symposium on Networked Systems Design and Implementation (NSDI)*. 1–18. Full-stack LLM training simulator achieving 98.1% alignment with real-world results. Alibaba Cloud/Tsinghua.
 [70] Zixian Wang et al. 2025. SynPerf: Synthesizing High-Performance GPU Kernels via Pipeline Decomposition. *arXiv preprint* (2025). Under review.
 [71] Samuel Williams, Andrew Waterman, and David Patterson. 2009. Roofline: An Insightful Visual Performance Model for Multicore Architectures. *Commun. ACM* 52, 4 (2009), 65–76. <https://doi.org/10.1145/1498765.1498785>
 [72] William Won, Taekyung Heo, Saeed Rashidi, Saeed Talati, Srinivas Srinivasan, and Tushar Krishna. 2023. ASTRA-sim2.0: Modeling Hierarchical Networks and Disaggregated Systems for Large-Model Training at Scale. In *Proceedings of the IEEE International Symposium on Performance Analysis of Systems and Software (ISPASS)*. 283–294. <https://doi.org/10.1109/ISPASS57527.2023.00035>
 [73] Yannan Nellie Wu, Joel Emer, and Vivienne Sze. 2022. Sparseloop: An Analytical Approach to Sparse Tensor Accelerator Modeling. In *Proceedings of the 55th IEEE/ACM International Symposium on Microarchitecture (MICRO)*. 1–15. <https://doi.org/10.1109/MICRO56248.2022.00078>
 [74] Gyeong-In Yu, Joo Seong Jeong, Geon-Woo Kim, Soojeong Kim, and Byung-Gon Chun. 2022. ORCA: A Distributed Serving System for Transformer-Based Generative Models. In *Proceedings of the 16th USENIX Symposium on Operating Systems Design and Implementation (OSDI)*. 521–538.
 [75] Geoffrey X. Yu, Yubo Gao, Pavel Golber, and Asaf Cidon. 2021. Habitat: A Runtime-Based Computational Performance Predictor for Deep Neural Network Training. In *Proceedings of the USENIX Annual Technical Conference (ATC)*. 503–521.
 [76] Yi Zhai, Yu Cheng Wang, Peng Jiang, and Congming Kang. 2023. TLP: A Deep Learning-based Cost Model for Tensor Program Tuning. In *Proceedings of the 28th ACM International Conference on Architectural Support for Programming Languages and Operating Systems (ASPLOS)*. 833–845. <https://doi.org/10.1145/3575693.3575736>
 [77] Li Lyra Zhang, Shihao Han, Jianyu Wei, Ningxin Zheng, Ting Cao, Yuqing Yang, and Yunxin Liu. 2021. nn-Meter: Towards Accurate Latency Prediction of Deep-Learning Model Inference on Diverse Edge Devices. In *Proceedings of the 19th Annual International Conference on Mobile Systems, Applications, and Services*

1625	(<i>MobiSys</i>). 81–93. https://doi.org/10.1145/3458864.3467882 Best Paper Award.	1683
1626	[78] Lianmin Zheng, Chengfan Jia, Minmin Sun, Zhao Wu, Cody Hao Yu, Ameer Haj-Ali, Yida Wang, Jun Yang, Danyang Zhuo, Koushik Sen, Joseph E. Gonzalez, and Ion Stoica. 2020. Ansor: Generating High-Performance Tensor Programs for Deep Learning. In <i>Proceedings of the 14th USENIX Symposium on Operating Systems Design and Implementation (OSDI)</i> . 863–879.	1684
1627		1685
1628	[79] Lianmin Zheng, Ruochen Liu, Junru Shao, Tianqi Chen, Joseph E. Gonzalez, Ion Stoica, and Zhihao Zhang. 2021. TenSet: A Large-scale Program Performance Dataset for Learned Tensor Compilers. In <i>Advances in Neural Information Processing Systems (NeurIPS)</i> , Vol. 34. 29876–29888.	1686
1629		1687
1630		1688
1631		1689
1632		1690
1633		1691
1634		1692
1635		1693
1636		1694
1637		1695
1638		1696
1639		1697
1640		1698
1641		1699
1642		1700
1643		1701
1644		1702
1645		1703
1646		1704
1647		1705
1648		1706
1649		1707
1650		1708
1651		1709
1652		1710
1653		1711
1654		1712
1655		1713
1656		1714
1657		1715
1658		1716
1659		1717
1660		1718
1661		1719
1662		1720
1663		1721
1664		1722
1665		1723
1666		1724
1667		1725
1668		1726
1669		1727
1670		1728
1671		1729
1672		1730
1673		1731
1674		1732
1675		1733
1676		1734
1677		1735
1678		1736
1679		1737
1680		1738
1681		1739
1682		1740